# Effects of Surface Roughness on the Diffusion Bonding of 2024 Aluminum Alloy

**Pei-Ing Lee[1], Shih-Ying Chang[2], Yu-Kai Sun[1], and Tung-Han Chuang[1*]**
[1] Department of Materials Science and Engineering, National Taiwan University, Taipei, Taiwan
leepeiing@gmail.com; changsy@yuntech.edu.tw; d03527003@ntu.edu.tw; tunghan@ntu.edu.tw
[2] Department of Mechanical Engineering, National Yunlin University of Science & Technology, 64002, Touliu, Yunlin, Taiwan
*Corresponding Author: tunghan@ntu.edu.tw

**Abstract -** The interfacial microstructure and shear strength properties of solid-state diffusion bonded 2024 aluminium alloy were investigated under varied surface roughness. The results indicated a high strength of 79.7 MPa for specimens electro-polished after diffusion bonding at 490°C for 120 min under pressure of 5 MPa, approximately 10 times above the minimally required shear strength of 7.9 MPa of the MIL-STD-883G specification. It was also found that the shear strength increased with increases in bonding temperature from 440°C to 490°C and bonding time from 30 to 240 min.

**Keywords:** Diffusion bonding, 2024 Aluminium alloy, shear strength, electro-polishing.

## 1. Introduction

Aluminum possesses the advantageous of light weight, high strength and, after anodic surface treatment, corrosion resistance. Among the various aluminum alloys, 2024 Al alloy is commonly used in the aeronautical industry due to its good mechanical properties and low cost. Aluminum alloys are usually bonded by fusion welding [1], such as tungsten gas shielded arc welding, melt inert-gas welding, laser welding and other technologies. However, fusion welding entails some problems. For example, fusion-welded base materials have large deformation and thermal zones, which are prone to cracking [2]. In addition, ceramic materials or high temperature materials cannot be bonded with Al alloys [3], and the resultant porosity is inappropriate for a vacuum chamber material [4]. Fusion welding also has a slow welding speed and high cost [5]; in addition, only butt bonding, and not face-to-face bonding, can be performed, and reactive metals cannot be heterogeneously bonded [6].

Another method of bonding Al alloys is brazing with the insertion of a filler metal having a melting temperature lower than that of the Al alloy. However, 2024 Al alloy has a low solidus temperature of 502°C, so it cannot be brazed using the traditional Al-12Si filler metal, which has a eutectic point of 577°C. Therefore, an alternative method for the joining of Al alloys may be diffusion bonding.

Diffusion bonding is a solid-state joining technique which involves heating the workpieces to high temperatures of 0.5 to 0.8 Tm (where Tm is the absolute melting temperature) under external pressure. In contrast to other joining techniques, such as fusion welding and brazing, diffusion bonding reduces the formation of brittle products and the thermal stress at the interface. Diffusion bonding can be performed without involving the liquid phase, and no additional materials are added [7]. The bond tends to exhibit the strength and heat resistance of the base material, and the bonding process causes no contamination [7]. In principle, it can be performed on any size of bonding surface without increasing the processing time [8]. It can also be used for the bonding of similar or dissimilar metals, or even refractory metals or materials of different thicknesses [9].

Diffusion bonding is commonly used in processes where material joining is difficult or impossible by other means. For example, it has been applied to welding materials that cannot be liquefied and fused, such as zirconium and beryllium, and materials with extremely high melting points, such as tungsten [10]. In addition, with solid-state diffusion bonding, heterogeneous metals can be bonded and strength can be maintained at high temperatures [10]. It has also been reported that diffusion bonding of aluminum alloys can effectively reduce porosity, cracks and weld deformation because the width

of the diffusion gradually increases and voids decrease as the temperature rises [11].

Diffusion bonding, which overcomes the problem of solidification cracking, has been applied to the production of high-integrity bonds of Cu alloys, stainless steels and Ti alloys. Moreover, diffusion bonding is a solid-state bonding process that is suitable for bonding thin plates and small parts with different geometries. The reasons are that it produces a bond surface without the material discontinuities formed in fusion or brazing workpieces and that the deformation of the bonded parts is minimal [12]. Diffusion bonding also provides a new bonding technique for similar and dissimilar materials without significant micro-deformation, and in homogeneous materials, few phase changes or microstructural changes occur during the bonding process [13]. Therefore, the material processing parameters, such as the bonding temperature, bonding pressure and bonding time, should be optimized to obtain a well-bonded interface. In addition, for modern engineering processes, lower bonding temperatures are necessary However, the formation of intermetallic compounds at a heterogeneous diffusion bonding interface is still an important issue that needs further attention. Recent studies have found that the addition of nanoparticles as a bonding interlayer has the potential to disrupt the intermetallic compounds while producing smaller grains that act internally to increase strength [14].

To date, diffusion bonding techniques have been successfully applied to aerospace superplastic titanium alloy structures, and the optimum conditions required to obtain high-quality diffusion bonds have been investigated using superplastic aluminum alloys [15, 16].

Although solid-state diffusion bonding of aluminum alloys has many advantages, the oxide film on the aluminum surface affects the metal-to-metal bonding [17]. Elsa, M., Khorram et al. [18] diffusion bonded Al/Cu with an intermediate layer of 100 $\mu$m Sn as the bonding aid layer, and an interfacial contact zone formed between the aluminum and copper surfaces along with the Sn interlayer. The Al-Cu-Sn precipitation phase also increased the bond strength. The shear strength of the Al/Cu bond was 78.39 MPa when the bonding pressure was increased to 5 MPa. Some studies have attempted to replace and prevent the re-formation of oxide films by using a liquid bonding aid layer as a flux [19]. For lower melting point aluminum alloys such as AA7075 and AA2024, however, the liquefaction effect may melt the bonding material, which is also a challenge for solid-state diffusion bonding of lower melting point aluminum alloys [20].

This research focused on the applicability of diffusion bonding of 2024 Al alloy and the optimal conditions for the bonding process. In addition, the effects of post-bonding heat treatments to improve the bonding strength were also examined.

## 2. Experimental

For the experiments, 2024 Al-T351 alloy plates with dimensions of 50 mm × 20 mm × 5 mm were employed, and the chemical composition is listed in Table 1. Electro-polishing was performed with an electrolyte of 70% $C_2H_5OH$, 15% $HClO_4$ and 15% $C_6H_{14}O_2$ at a working voltage of 15 V for 10 min. For comparison, certain specimens were ground with 1000 and 2000 grit silicon carbide sandpaper. After the surface treatments, the specimens were stacked and placed in a hot press vacuum furnace as illustrated in Fig. 1. Diffusion bonding was conducted at temperatures ranging from 440°C to 490°C for 30 min to 240 min under external pressure of 5 MPa. To enhance the bonding strength, certain specimens diffusion-bonded at 450°C, 470°C, and 490°C for 240 min were further heated at 450°C for 1 h, quenched in water to room temperature (T4 treatment), and then aged at 191 °C for 12 h (T6 treatment).

The diffusion bonded specimens were ground and polished before observation by scanning electron microscopy (FEG-SEM, NOVA NANO SEM 450). The chemical composition of the precipitates which formed at the interface and in the matrix were analyzed with energy dispersive X-ray analysis (EDX). Bond shear strength was measured by cupping machine at room temperature. The fractography of the specimens after shear tests was also observed by SEM. The microhardness across the bonding interface of the bonded specimens was measured in accordance with ASTM E384. The measurement position was at the approximate center of the bonded specimen, the hardness was measured at 0.1 mm intervals at each point, and the measurement range extended from the center of the bonded interface to the left and right.

Table 1 The chemical composition of Al2024 aluminum alloy (wt.%).

| Al | Cu | Mg | Mn | Si | Fe | Zn | Ti |
|------|------|------|------|------|------|------|------|
| Bal. | 4.61 | 1.41 | 0.50 | 0.05 | 0.12 | 0.15 | 0.02 |
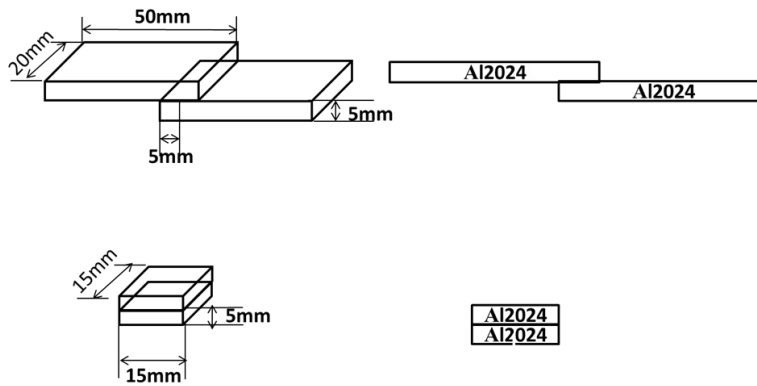
Fig. 1 Experimental solid-state diffusion bonding of AA 2024 specimens and schematic diagram of the bonding process.

## 3. Results and Discussion
### 3.1. Surface characterization

The surface roughness values of the Al 2024 surfaces with various surface treatments were measured by atomic force microscopy (AFM) and are listed in Table 2. The surface parameter, $R_a$, represents the arithmetical mean roughness of the profile height deviations from the mean line. As expected, the alloy surface ground using the P2000 grit SiC sandpaper had the roughest surface, while the electropolished surface exhibited the smoothest of all the surfaces.

Table 2 Surface roughness of Al 2024 surfaces with different surface treatments.

| Parameter | Untreated | P2000 grit | Electropolished |
|---|---|---|---|
| $R_a$ (µm) | 0.38 | 0.67 | 0.22 |

Fig. 2 shows the surface morphologies of the Al 2024 alloy treated with different surface treatments. It was observed that the specimen ground wtih P2000 grit exhibited more obvious microscopic scratches of greater depth than those of the untreated surface, which was consistent with the measured values in Table 2. Meanwhile, the electropolished specimen exhibited a mirror-like polished surface with no visible scratches.
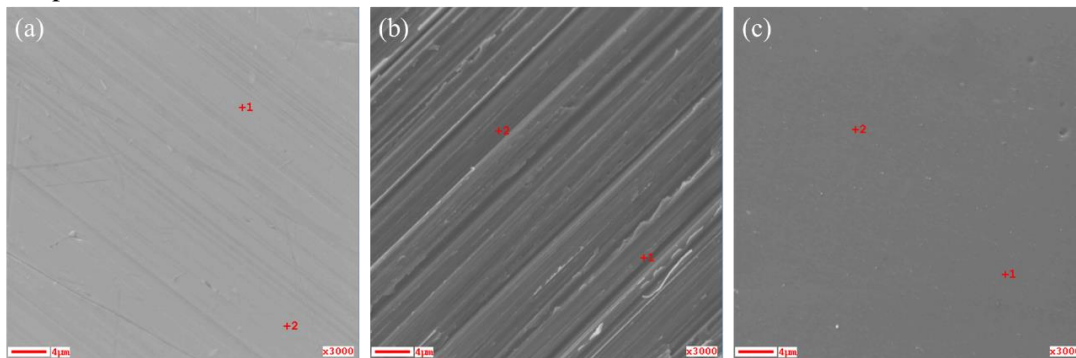


Fig. 2 Surface morphologies of Al 2024 surfaces after various surface treatments (a) untreated (b) ground with P2000 grit SiC sandpaper (c) electropolished.

### 3.2. Diffusion Bonding

The specimens were further examined with a differential thermal analyzer (DMA) to identify the thermal properties of the Al 2024 alloy. According to the heat flow scan in Fig. 3, Al 2024 alloy has a liquidus temperature of 511 °C. Hence, to maintain the structural and mechanical integrity of the joints, the bonding temperatures were set below the liquidus temperature (450°C, 470°C and 490°C) to avoid any liquid formation. Since oxides formed on the alloy surface can be detrimental to the bonding of the joints, the oxidation on the surface of the aluminium alloy was eliminated to fully

investigate the influence of surface quality on adhesive strength. Fig. 4 displays the AES analysis plots of Al 2024 after various surface treatments. With a drastic decrement in oxygen content across the depth length, the alloy exhibited a thin oxide layer (< 1 μm) on the surface after all surface treatments. Hence, the development of a bonding method to disrupt the oxide layer would lead to significant enhancement of the bond integrity.
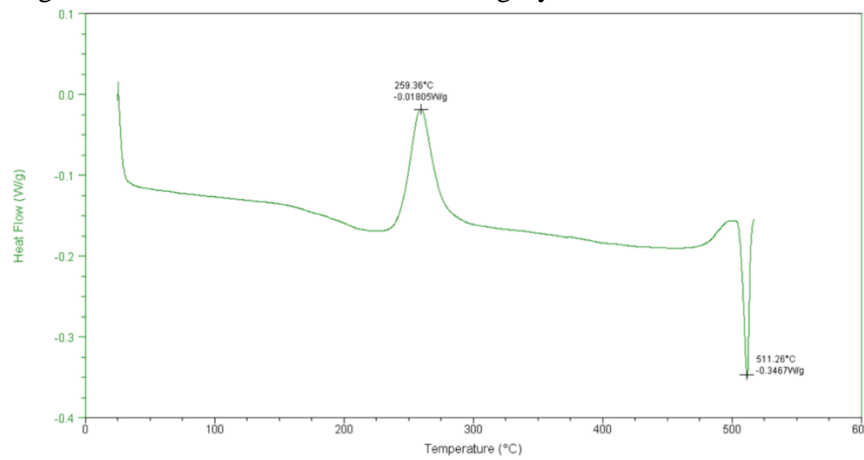


Fig. 3 Heat flow scan of Al 2024 alloy.
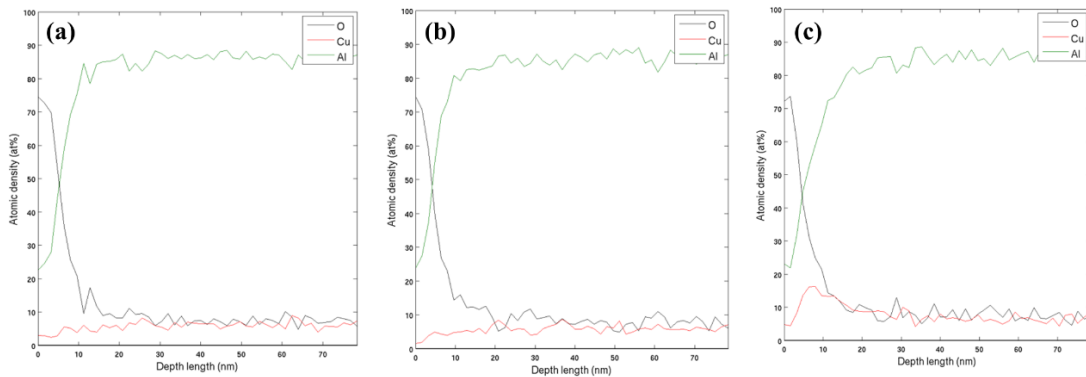


Fig. 4 AES depth profile analysis of Al 2024 surfaces after various surface treatments (a) untreated (b) ground with P2000 grit SiC sandpaper (c) electropolished.

In general, it is believed that smoother surfaces will yield a joint with higher bond strength due to better diffusion during the bonding process. Fig. 5 shows the microstructures of joints ground with P2000 grit and diffusion bonded at 450°C to 490°C for a constant bonding time of 30 min. The bonding interfaces for all temperatures are indicated by white arrows. In fact, the brittle and continuous oxide layer that formed on the alloy surface was disrupted by the substantial plastic deformation resulting from the diffusion bonding process. Under a static bonding pressure of 5 MPa and a holding time of 30 min, the extensive oxide rupture, caused by the large amount of plastic deformation, allowed metal-to-metal contact of the alloy surfaces to form metallurgical bonds. Also, it is notable that the better bonding integrity was reflected in the invisible bonding interfaces at bonding temperatures of 470°C and 490°C, as shown in Fig. 4(b) and 4(c). The bonding process at 450°C failed to produce a sound bonding interface, leaving a continuous gap between the bonded specimens. This gap was bridged only at irregular intervals by regions where only limited localized bonding had taken place, leaving large voids at the bond interface. The results clearly indicated that the bonding temperature of 450°C was too low for successful bonding, as the elements in the alloy were not soluble to each other. This led to a large amount of the intermetallic compound Al-Cu-Mg forming at the bonding interface, which was the main factor in the poor bond strength. As the solubility of the alloy increased with increasing temperature, higher bonding temperatures promoted better bonding integrity for diffusion bonding.
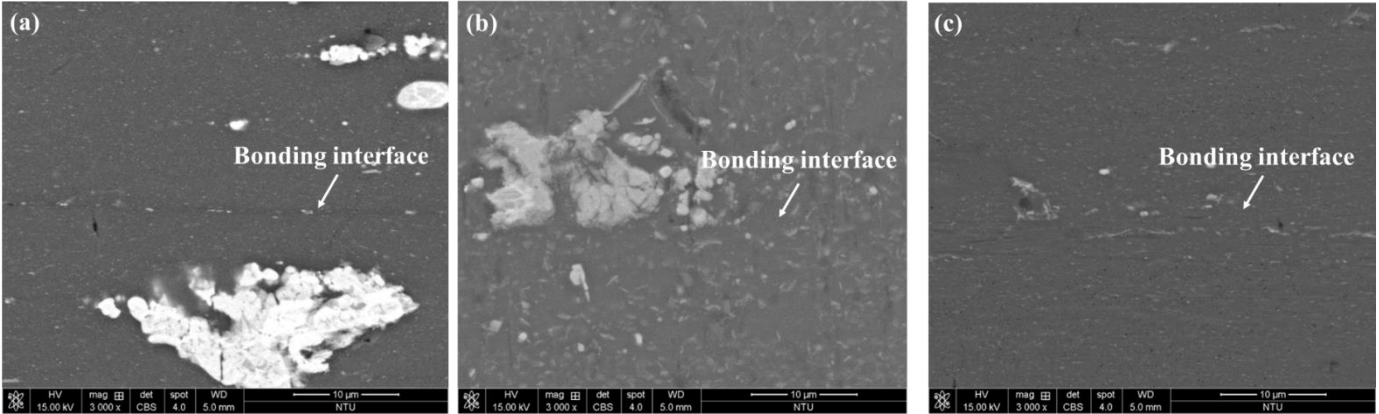
Fig. 5 Interface of Al 2024 ground with P2000 grit SiC sandpaper for 30 min and bonded at (a) 450°C (b) 470°C and (c) 490°C.

In contrast, the low temperature diffusion bonding of Al 2024 with electropolished surfaces showed significant enhancement of the bond integrity with decreases in surface roughness. This enhancement indicated that the use of a surface treatment to create a smooth continuous surface yielded better bond integrity. As shown in Fig. 6, the bonding interface was difficult to observe due to the similarity in composition of the base metal and the sound metallurgical bond that formed. Since the base materials were identical, mutual diffusion dominated, so no interlayer of intermetallic compounds (IMC) formed between the facing surfaces. A closer look at the bonding interface is provided in Fig. 7. The microstructure of the electropolished bonding interface revealed a straight interface grain boundary. Apparently, no voids formed in the bonding interface at any of the bonding temperatures. Additionally, in comparison with the grain size at 450°C (Fig. 7a), the grain growth was obvious at elevated temperature. If grain growth is rather severe at higher temperatures during the bonding process, softening of the base material is likely to occur.
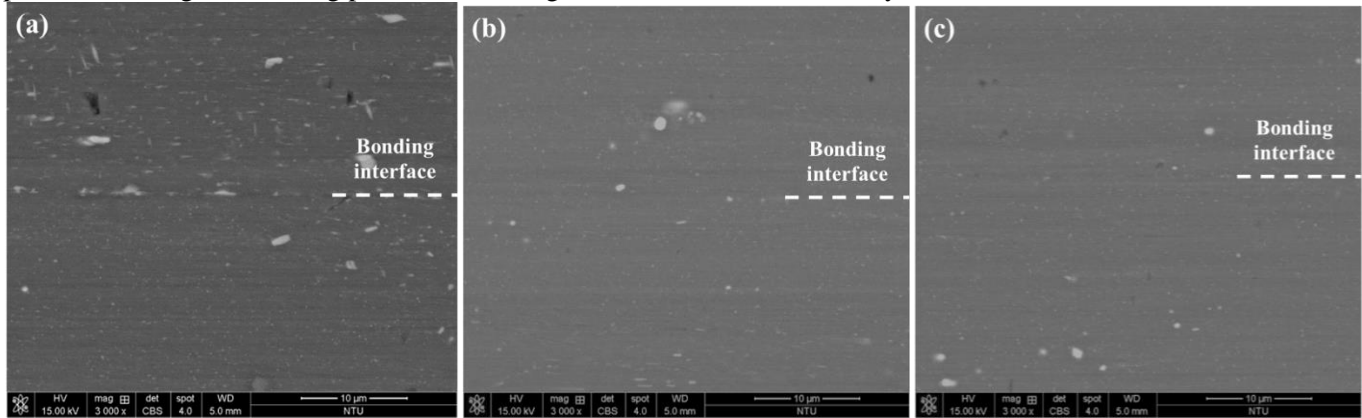


Fig. 6 Interface of electropolished Al 20240 bonded for 30 min at (a) 450°C (b) 470°C and (c) 490°C.
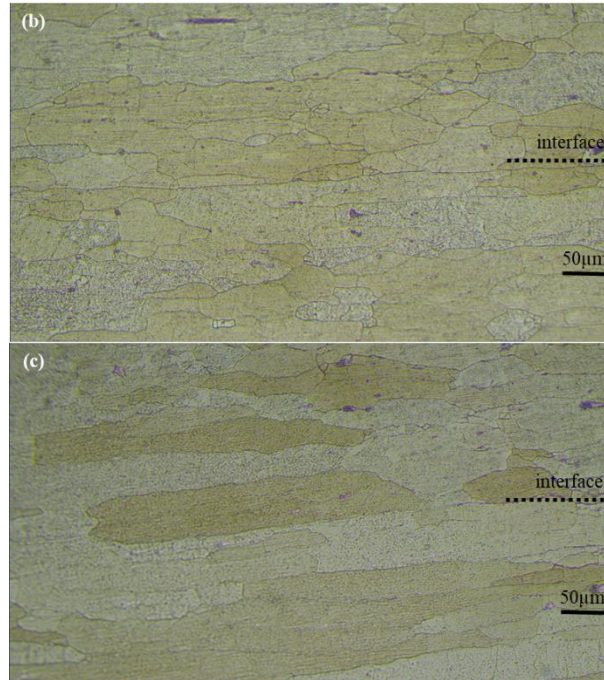
Fig. 7 Microstructural view of the electropolished Al 2024 interfaces bonded for 30 min at (a) 450°C (b) 470°C and (c) 490°C.

## 2.4. Tensile Properties

The surface morphology of the shear-fractured sample diffusion bonded at 490 °C for 30 min is shown in Fig. 8. The average joint shear strength was 71.6 MPa. The fractography of both sides of the specimen featured flat fracture with numerous voids and dimples distributed on the fracture surface. The flat fracture surface indicated brittle fracture and a low shear strength of the joint. More shear dimples were observed on the top side of the fracture surface, indicating that the fracture mode of the joint was ductile fracture, with strong metallic bonds formed in the localized area. Fig. 8(b) shows that the dimples were in a similar direction on the surface, implying that the failure was caused by plastic deformation under extensive slip on the activated slip planes. The chemical compositions of points A and B, determined by EDX analysis, revealed that the chemical compositions of the fracture surfaces were mainly similar. The findings can be explained by considering the bonding temperature of 490 °C, which was close to the melting point of the base material. The elements uniformly dissolved into the base metal, resulting in solid solution strengthening at the joint.
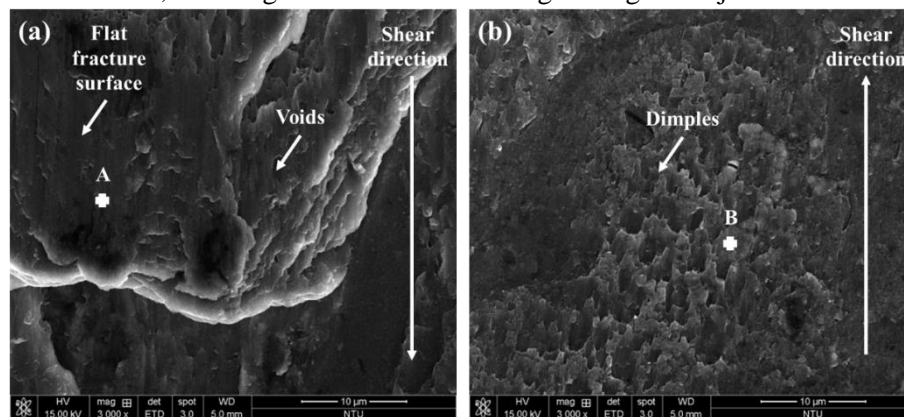


Fig. 8 Fractography of electropolished Al 2024 joint bonded at 490 °C for 30 min (a) bottom side (b) top side.

Prolonging the bonding period contributed to fluctuations in the bonding strength of the diffusion bonded Al 2024 joints with different surface preparations, as plotted in Fig. 9. All the diffusion bonded Al 2024 joints showed a rising trend

with prolonged bonding periods, while the highest bonding strength of 181.5 MPa was found in the specimen diffusion bonded at 490 °C for 240 min. Due to the absence of defects and brittle IMC phase in the interface, the diffusion bonding method was expected to provide excellent bond integrity. More elongated and equiaxed dimples were distributed over the fracture surface, as shown in Fig. 10, implying the high plasticity of the material and strong metallurgical bonds. In fact, the fractography analysis suggested that increasing the bonding period could significantly promote more metallurgical bonding, resulting in higher joint strength. However, the measured bonding strength did not provide sufficient evidence of successful bonds in the electropolished Al 2024 joints.
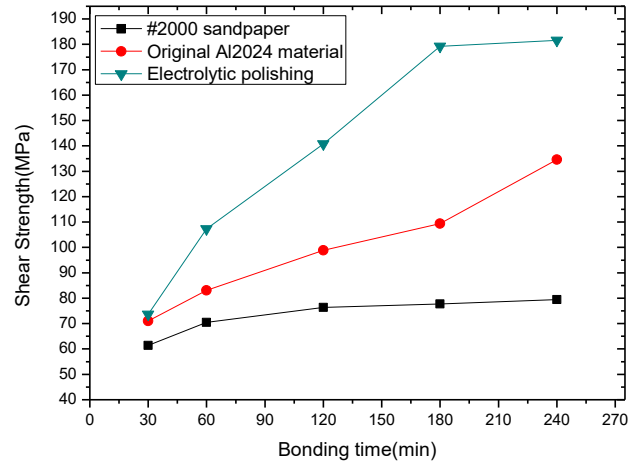


Fig. 9 Bonding strength of Al 2024 joints diffusion bonded at 490 °C for 30–240 min.
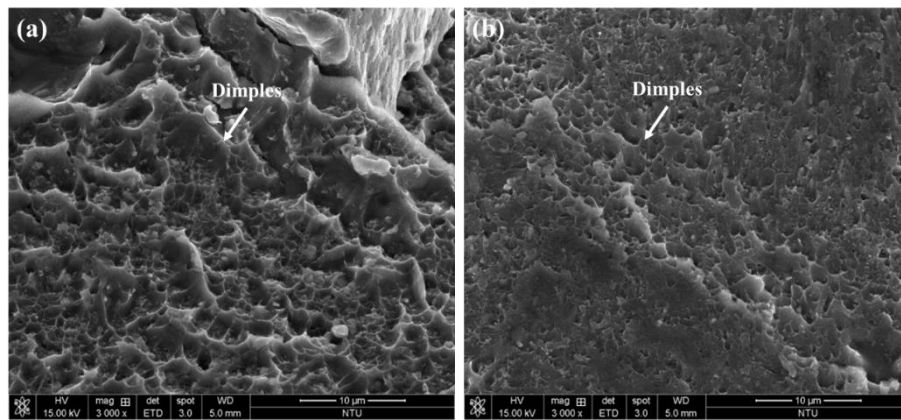


Fig. 10 Elongated dimples formed on the fracture surfaces of Al 2024 joint bonded at 490 °C for 240 min: (a) bottom side (b) top side.

## 4. Conclusions

This paper has presented the effects of surface roughness on the integrity of aluminium alloy 2024 bonds fabricated by diffusion bonding. It was found that the joints with electropolished surfaces yielded bonds of higher integrity than those of the specimens with surfaces prepared by other methods. The shear strength of the joints ranged from 62.5 MPa to 181.5 MPa with increases in the bonding period from 30 to 240 min. The maximum shear strength of 181.5 MPa was obtained by bonding at 490 °C for 240 °C under 5MPa. The fractographs revealed an enlarged dimple zone, and the fracture surfaces displayed a typical ductile fracture mode after the prolonged bonding period. Ideal diffusion bonding can be achieved when the bonding interface is free of both defects and the brittle IMC phase, which can be detrimental to the bond integrity.

## Acknowledgement

## References

[1] Kuhlmann, A. M. (1963). The second most abundant element in the earth's crust. JOM, 15(7), 502-505.

[2] Abd El-Hameed, A. M., & Abdel-Aziz, Y. A. (2021). Aluminium Alloys in Space Applications: A Short Report. J. Appl. Sci. Eng., 22(1), 1-7.

[3] Deepati, A. K., Alhazmi, W., & Benjeer, I. (2021). Mechanical characterization of AA5083 aluminium alloy welded using resistance spot welding for the lightweight automobile body fabrication. Mater T :P, *45*, 5139-5148.

[4] B. Çevik, M. Koç, The effects of welding speed on the microstructure and mechanical properties of marine-grade aluminium (AA5754) alloy joined using MIG welding, Kov. Mater. 57 (2019) 307–316,

[5] Tung, S. K., & Lim, L. C. (1994). Void formation in wide gap brazing usingprepacks of nickel base braze mixes. J Mater Sci Technol, 10(5), 364 369.

[6] Koprivica, A., Bajić, D., Šibalić, N., & Vukčević, M. (2020). Analysis of welding of aluminium alloy AA6082-T6 by TIG, MIG and FSW processes from technological and economic aspect. Mach. Technol. Mater., *14*(5), 194-198.

[7] Peng, L., Yajiang, L., Haoran, G., & Juan, W. (2006). Investigation of interfacial structure of Mg/Al vacuum diffusion-bonded joint. Vacuum, 80(5), 395-399.

[8] Choudhary, A. K., & Jain, R. (2021). Fundamentals of Friction Stir Welding, Its Application, and Advancements. Weld T, 41-90.

[9] A. Heidarzadeh, S. Mironov, R. Kaibyshev, G. Çam, A. Simar, A. Gerlich, F. Khodabakhshi, A. Mostafaei, D.P. Field, J.D. Robson, A. Deschamps, P. J. Withers, Friction stir welding/processing of metals and alloys: a comprehensive review on microstructural evolution, Prog. Mater. Sci. 117 (2021), 100752.

[10] Bang, H. S., Hong, S. M., Das, A., & Bang, H. S. (2021). Study on the weldability and mechanical characteristics of dissimilar materials (Al5052-DP590) by TIG assisted hybrid friction stir welding. Met. Mater. Int., *27*(5), 1193-1204.

[11] Majeed, T., Mehta, Y., & Siddiquee, A. N. (2021). Analysis of tool wear and deformation in friction stir welding of unequal thickness dissimilar Al alloys. Proc. Inst. Mech. Eng. L, *235*(3), 501-512.

[12] Li, G., Jiang, W., Guan, F., Zhu, J., Zhang, Z., & Fan, Z. (2021). Microstructure, mechanical properties and corrosion resistance of A356 aluminum/AZ91D magnesium bimetal prepared by a compound casting combined with a novel Ni-Cu composite interlayer. J Mater Process Technol, 288,116874.

[13] Li, G., Jiang, W., Yang, W., Jiang, Z., Guan, F., Jiang, H., & Fan, Z. (2019). New insights into the characterization and formation of the interface of A356/AZ91D bimetallic composites fabricated by compound casting. Metall Mater Trans A, 50(2), 1076-1090.

[14] Li, G., Yang, W., Jiang, W., Guan, F., Jiang, H., Wu, Y., & Fan, Z. (2019). The role of vacuum degree in the bonding of Al/Mg bimetal prepared by a compound casting process. J Mater Process Technol, 265, 112-121.

[15] Burkhart, E. T., & Hefti, L. (2020). Advancements of Superplastic Forming and Burkhart, E. T., & Hefti, L. (2020). Advancements of Superplastic Forming and Diffusion Bonding of Titanium Alloys for Heat Critical Aerospace Diffusion Bonding of Titanium Alloys for Heat Critical Aerospace Applications. SAE Tech. Pap, 2 (2020Applications. SAE Technical Paper, 2(2020--0101--0033).0033).

[16] Bhatta, L., Pesin, A., Zhilyaev, A. P., Tandon, P., Kong, C., & Yu, H. (2020). Recent development of superplasticity in aluminum alloys: A review. Metals, 10(1), 77.

[17] Sajan, M., Sampatirao, H., Balasubramanian, R., & Nagumothu, R. (2021). Plasma electrolytic oxidation of AZ31 magnesium alloy diffusion bonded with aluminium. Mater T :P.

[18] AlHazaa, A., Haneklaus, N., & Almutairi, Z. (2021). Impulse pressure-assisted diffusion bonding (IPADB): Review and outlook. Metals, 11(2), 323.

[19] Shioga, T., Mizuno, Y., & Nagano, H. (2020). Operating characteristics of a new ultra-thin loop heat pipe. Int. J. Heat Mass Transf., 151, 119436.

[20] Zhang, C., Li, H., & Li, M. Q. (2015). Formation mechanisms of high quality diffusion bonded martensitic stainless steel joints. Sci. Technol. Weld. Join., 20(2), 115-122.

[21] AlHazaa, A., Khan, T. I., & Haq, I. (2010). Transient liquid phase (TLP) bonding of Al7075 to Ti–6Al–4V alloy. Mater Charact, 61(3), 312-317.

[22] ASTM E 384. (2008). Test Method for Microindentation Hardness of Materials.

[23] Nao Osawa. (2010). Introduction to Illustrated Basics and Mechanisms of Aluminum. Shuwa System. ISBN 9784798025063

[24] Jiang X J, Nobel B, Hansen B, et a1, Metall Trans A, 2001, 32(5), 1063.

[25] C. R. Barrett, W. D. Nix and A. S. Tetelman(1973). The prin-ciples of Engineering Materials. Prentice-Hall Inc

[26] Mondolfo, L. F. (1976). Aluminum Alloys: Structure and Properties. London: Butter Worths.